Open Access
Original paper

Budownictwo i Architektura / Civil and Architectural Engineering 25(3) (2026) 26042
https://doi.org/10.35784/bud-arch.8893

Structural response of circular RC elements under nonlinear hereditary creep

Mukhlis Hajiyev[1], Ulviya Hajiyeva[2], Seymur Bashirzade[3,*], Baxrom Xasanov[4]

[1] *Azerbaijan University of Architecture and Construction, Baku, Azerbaijan; hajiyevmukhlis60@gmail.com*
[2] *Azerbaijan University of Architecture and Construction, Baku, Azerbaijan*
[3] *Azerbaijan University of Architecture and Construction, Baku, Azerbaijan; srbashirzade@gmail.com*
4 *Tashkent Institute of Architecture and Construction, Tashkent, Uzbekistan; b.xasanov@taqu.uz*

[*] *Corresponding Author*
Received: 17.12.2025; Revised: 23.06.2026; Accepted: 23.06.2026; Available online: 31.07.2026

Abstract:
This study presents an efficient methodology for analysing the stress–strain state and load-bearing capacity of circular reinforced concrete columns under short- and long-term loading conditions. The proposed approach incorporates the nonlinear hereditary creep of concrete and the elastic–plastic behaviour of reinforcement, enabling accurate predictions without the need to classify elements as "short" or "long" or to separately account for eccentricity. A discrete analogue of the nonlinear hereditary creep integral equation was formulated and solved using a robust computational algorithm, which was validated through parametric studies. The findings indicate that time-dependent creep has a pronounced influence on structural performance, leading to a noticeable reduction in load-bearing capacity and highlighting the importance of considering these effects in design and analysis. The methodology ensures engineering-level accuracy, even for large time steps, and provides a unified framework for evaluating the deformation, stability, and parameter sensitivity of reinforced concrete structures.

Keywords:
reinforced concrete; circular cross-section; nonlinear hereditary creep; stress–strain analysis; load-bearing capacity; long-term effects; numerical modelling

1. Introduction

In recent years, the development of calculation methodologies based on nonlinear deformation models for reinforced concrete (RC) structures has gained significant attention [4,7]. Modern construction standards increasingly recommend the use of nonlinear models to achieve more accurate predictions of structural behaviour under load and optimise the utilisation of material strength reserves [3]. Comparative studies of international design codes have confirmed the necessity of incorporating such models into the analysis and design of reinforced concrete elements [3,7]. Consequently, these models have found wide application in engineering practice [6]. For circular cross-section compressed elements, deriving simple analytical formulas is generally not feasible because of the complexity of their stress–strain behaviour. Therefore, efficient numerical techniques are considered the most appropriate approach [1,2,8,9]. The challenge becomes even more pronounced when accounting for the nonlinear hereditary creep of concrete under long-term loading conditions, which significantly influences the structural performance [5,7,11-16]. Long-term creep effects have been extensively studied in various contexts, including high-performance concrete [11], prestressed concrete beams [12], and recycled aggregate concrete [14]. Experimental investigations and modelling approaches have consistently demonstrated that creep alters deformation characteristics and reduces structural resistance over time [12,15,17]. Furthermore, advanced predictive models, including machine learning-based approaches, have been proposed to evaluate the factors affecting creep behaviour [16]. Similar time-dependent phenomena have been observed in other engineering materials, such as polyamide ropes used in mooring applications, emphasising the universal importance of creep in structural design [10]. Circular RC columns serve as primary load-bearing elements in numerous engineering applications, such as in building columns and bridge piers. These elements are predominantly subjected to axial compression and, in some cases, combined compression and bending. Consequently, their stress–strain state and load-bearing capacity must be analysed by considering the simultaneous action of axial and transverse forces. However, the lack of straightforward formulas for such evaluations is primarily due to the problem's mathematical complexity. Even under short-term static loading, when creep is neglected, the solution remains challenging. This complexity underscores the necessity of applying nonlinear deformation models to accurately determine the load-bearing capacity and structural stability [13,14]. This study addresses these challenges by proposing an advanced numerical methodology that incorporates nonlinear hereditary creep effects and the elastic–plastic behaviour of reinforcement. This approach provides a unified framework for analysing both short- and long-term loading scenarios, ensuring engineering-level accuracy and practical applicability for modern reinforced concrete designs.

2. Problem statement

When RC elements are subjected to long-term loading, concrete creep becomes critical. To accurately describe this phenomenon, the nonlinear hereditary creep of concrete is expressed by the following integral equation [18]:

$$\varepsilon_b(t) = \frac{1}{E(t)} \cdot U(\sigma_b(t)) - \int_{t_0}^{t} V(\sigma_b(\tau)) \cdot K(t,\tau)\, d\tau \qquad (1)$$

This equation considers both instantaneous and long-term deformations, which are approximated using nonlinear functions [18]:

$$U\left(\sigma_b(t)\right)=\sigma_b(t)\cdot\left[1+\eta_1\cdot\left(\frac{\sigma_b(t)}{R_b}\right)^{m_1}\right]$$

$$V\left(\sigma_b(\tau)\right)=\sigma_b(\tau)\cdot\left[1+\eta_2\cdot\left(\frac{\sigma_b(\tau)}{R_b}\right)^{m_2}\right]$$

$$K(t,\tau)=\frac{\partial}{\partial\tau}\left(\frac{1}{E(\tau)}-\frac{1}{E(t)}+C(t,\tau)\right) \tag{2}$$

Here, denotes the basic creep parameter. To make the solution practical for engineering applications, the integral equation is transformed into a discrete analogue:

$$\varepsilon_n=\frac{1}{E_n}\cdot U(\sigma_n)-\frac{\tau_n-\tau_{n-1}}{6}\cdot\left(K_{n,n}+2\cdot K^*_{n,n}\right)\cdot V(\sigma_n)-W_n \tag{3}$$

In this form, the term W_n accounts for the stress–strain state accumulated during previous time steps and is calculated as:

$$\begin{aligned}W_n=&-\frac{\tau_1-\tau_0}{6}\cdot\left[V(\sigma_0)\cdot\left(K_{n,0}+2\cdot K^*_{n,1}\right)+V(\sigma_1)\cdot\left(K_{n,1}+2\cdot K^*_{n,1}\right)\right]-\\&-\frac{\tau_2-\tau_1}{6}\cdot\left[V(\sigma_1)\cdot\left(K_{n,1}+2\cdot K^*_{n,2}\right)+V(\sigma_2)\cdot\left(K_{n,2}+2\cdot K^*_{n,2}\right)\right]-....-\\&-\frac{\tau_k-\tau_{k-1}}{6}\cdot\left[V(\sigma_{k-1})\cdot\left(K_{n,k-1}+2\cdot K^*_{n,k}\right)+V(\sigma_k)\cdot\left(K_{n,k}+2\cdot K^*_{n,k}\right)\right]-...\\&-\frac{\tau_{n-1}-\tau_{n-2}}{6}\cdot\left[V(\sigma_{n-2})\cdot\left(K_{n,n-2}+2\cdot K^*_{n,n-1}\right)+V(\sigma_{n-1})\cdot\left(K_{n,n-1}+2\cdot K^*_{n,n-1}\right)\right]-\\&-\frac{\tau_n-\tau_{n-1}}{6}\cdot\left(K_{n,n-1}+2\cdot K^*_{n,n-1}\right)\cdot V(\sigma_{n-1})\end{aligned} \tag{4}$$

As a result, solving the original integral equation reduces to solving a system of nonlinear algebraic equations for different time intervals. To verify the accuracy of this approach, a relaxation problem was analysed. For this purpose, the following expression for the basic creep criterion was adopted:

$$\begin{aligned}&C(t,\tau)=\phi(\tau)-\frac{\phi(t)-\Delta(t)}{e^{\gamma\cdot t}-A_2}\cdot\left(e^{\gamma\cdot\tau}-A_2\right)-\Delta(\tau)\cdot e^{-\alpha\cdot(t-\tau)}\\&\phi(\tau)=\phi_0+\phi_1\cdot e^{-\beta_1\cdot\tau}+\phi_2\cdot e^{-\beta_2\cdot\tau}+\phi_3\cdot e^{-\beta_3\cdot\tau}+...\\&\Delta(\tau)=\Delta_0+\Delta_1\cdot e^{-\alpha_1\cdot\tau}+\Delta_2\cdot e^{-\alpha_2\cdot\tau}+\Delta_3\cdot e^{-\alpha_3\cdot\tau}+...\end{aligned} \tag{5}$$

3. Parametric study 1. stress–relaxation behaviour of concrete

To implement the proposed methodology, the parameters included in the creep expression were selected based on experimental and normative data [19]. For the adopted creep model, the following values were considered:

$$\phi_0=24.5\cdot10^{-6}\ (\mathrm{MPa})^{-1}$$

$$\phi_1=10.0\cdot10^{-6}\ (\mathrm{MPa})^{-1}$$

$$\phi_2=43.2\cdot10^{-6}\ (\mathrm{MPa})^{-1}$$

$$\phi_3=35.0\cdot10^{-6}\ (\mathrm{MPa})^{-1}$$

$$\beta_1=0.023$$

$$\beta_2=0.1275$$

$$\beta_3=0.350$$

$$\Delta_0=11.2\cdot10^{-6}\ (\mathrm{MPa})^{-1}$$

$$\Delta_1=34.0\cdot10^{-6}\ (\mathrm{MPa})^{-1}$$

$$\alpha_1=0.125$$

$$\alpha=5$$

$$\gamma=0.02$$

$$A_2=0.85$$

For concrete of class B30, the nonlinear parameters were taken as: η_1 =1.3, m_1 = 4.3, η_2 =1.6, m_2 = 4.0, $E_b(\tau)=E_{b0}\cdot\left(1-\alpha_E\cdot e^{-\beta_E\cdot\tau}\right)$. The nonlinear parameters were adopted as η_1 =1.3, m_1 = 4.3, η_2 =1.6, and m_2 = 4.0 based on experimental data and normative codes. The variation of the elastic modulus over time was assumed according to a predefined function $E_b(\tau)=E_{b0}\cdot\left(1-\alpha_E\cdot e^{-\beta_E\cdot\tau}\right)$, reflecting the gradual reduction of stiffness due to creep. In parametric calculations, the initial elastic modulus and the time-dependent factor α_E = 0.573 and β_E = 0.063(day)$^{-1}$ were set to value consistent with standard design practices.

To solve the relaxation problem, a dedicated computational module was developed. This program was used to perform a series of parametric studies, and the results of selected cases are presented in the following figures.

Figure 1 shows the stress relaxation curves obtained from numerical simulations at different initial stress levels and time increments. The primary objective of this analysis was to validate the accuracy and stability of the proposed numerical algorithm for solving the discrete analogue of the nonlinear hereditary creep equation.

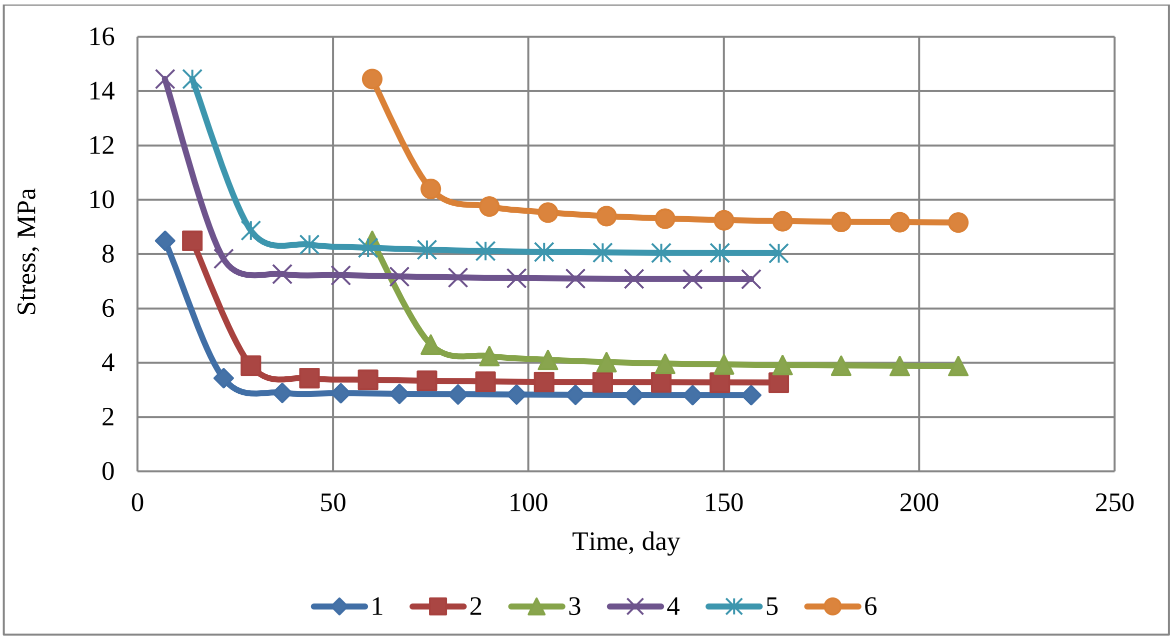

Fig. 1. Stress-relaxation relationship concrete: 1 - $\sigma_b = 0.5R_b$; $t_0 = 7$ day, 2 - $\sigma_b = 0.5R_b$; $t_0 = 4$ day, 3- $\sigma_b = 0.5R_b$; $t_0 = 60$ day, 4 - $\sigma_b = 0.85R_b$; $t_0 = 7$ day, 5 - $\sigma_b = 0.85R_b$; $t_0 = 14$ day, 6- $\sigma_b = 0.85R_b$; $t_0 = 60$ day

The results indicate that increasing the time step from the minimum value to the maximum considered in the study leads to a difference of less than 3% in the final relaxed stress values. This finding demonstrates that the algorithm maintains high precision even with relatively large time increments, which is essential for practical engineering applications where computational efficiency is critical.

Another important observation is the significant influence of concrete age and initial loading level on the relaxation process. For instance, when the initial stress corresponds to 50% of the compressive strength of concrete, the final relaxed stress values for the selected time intervals were approximately $\sigma_{b(7)}(\infty) = 2.812$ MPa, $\sigma_{b(14)}(\infty) = 3.273$ MPa, and $\sigma_{b(60)}(\infty) = 3.884$ MPa. In contrast, when the initial stress is increased to 85% of the compressive strength, the corresponding final values rise to $\sigma_{b(7)}(\infty) = 7.079$ MPa, $\sigma_{b(14)}(\infty) = 8.037$ MPa, and $\sigma_{b(60)}(\infty) = 9.164$ MPa. These results clearly show that higher initial stress levels lead to greater residual stress after relaxation, while younger concrete exhibits more pronounced creep effects.

The trends shown in Fig. 1 are evident: the curves exhibit a steeper initial decline in stress for younger concrete and higher initial stress levels, indicating rapid creep development during the early stages of loading. Over time, the curves gradually stabilised, reflecting the progression of the material toward a long-term equilibrium state. These observations confirm that the proposed approach provides both accuracy and robustness. Furthermore, they emphasised the critical importance of incorporating time-dependent phenomena, such as creep, into the design and structural assessment of RC elements.

4. Problem statement for long-term loading analysis

In this section, we analyse the stress–strain state of circular cross-section RC elements subjected to long-term loading, considering the nonlinear creep of concrete. This phenomenon significantly affects the deformation and internal force distribution within compressed RC members, particularly columns and piers, which are widely used in structural systems. According to the nonlinear deformation theory of RC and research by V.M. Bondarenko, the distribution of compressive stress across the concrete section cannot be assumed to be linear. Instead, it follows a nonlinear law that reflects the actual behaviour of concrete under high stress levels and sustained load. The stress distribution is expressed as [18]:

$$\sigma_{bz} = \sigma_b \cdot \left(\frac{z + x - R}{x}\right)^{n_\sigma} \tag{6}$$

Here, the fullness coefficient of the compressive stress diagram is defined as $n_\sigma = 1 - (1 - f_0) \cdot \left(\frac{\sigma_b}{R_b}\right)^{m_\sigma}$ [18]. For calculations, it can be taken as $m_\sigma = 2m_1/3$ for heavy concrete and $f = 0.11$ for lightweight concrete [18]. Based on the above, the following expressions can be written for the internal axial force and bending moment formed by the normal compressive stresses in the concrete section:

$$N_b(\sigma_b, x) = 2\sigma_b \cdot \int_q^R \left(\frac{z + x - R}{x}\right)^{n_\sigma} \cdot \sqrt{R^2 - z^2}\, dz \tag{7}$$

$$M_b(\sigma_b, x) = 2\sigma_b \cdot \int_q^R \left(\frac{z + x - R}{x}\right)^{n_\sigma} \cdot z \cdot \sqrt{R^2 - z^2}\, dz \tag{8}$$

Depending on the position of the neutral axis (Fig. 2), the lower limit of the integral is defined accordingly $q = \begin{cases} -R, & \text{if } x \geq 2R \\ R - x, & \text{if } 0 < x < 2R \end{cases}$. Similarly, assuming that the reinforcing bars deform according to a bilinear stress–strain diagram, the stress in any j-th reinforcement bar can be expressed as follows:

$$\sigma_{s,j}\left(\varepsilon_b, x\right)=\begin{cases} E_{s,j}\cdot\dfrac{\varepsilon_b}{x}\cdot\left(R_{s,j}\cdot\sin\phi_{s,j}+x-R\right);\, if & \left|\dfrac{\varepsilon_b}{x}\cdot\left(R_{s,j}\cdot\sin\phi_{s,j}+x-R\right)\right|\le\varepsilon_{s,ax} \\ R_{s,j}\cdot sign\left(\dfrac{\varepsilon_b}{x}\cdot\left(R_{s,j}\cdot\sin\phi_{s,j}+x-R\right)\right);\, if & \left|\dfrac{\varepsilon_b}{x}\cdot\left(R_{s,j}\cdot\sin\phi_{s,j}+x-R\right)\right|\le\varepsilon_{s,ax} \end{cases} \tag{9}$$

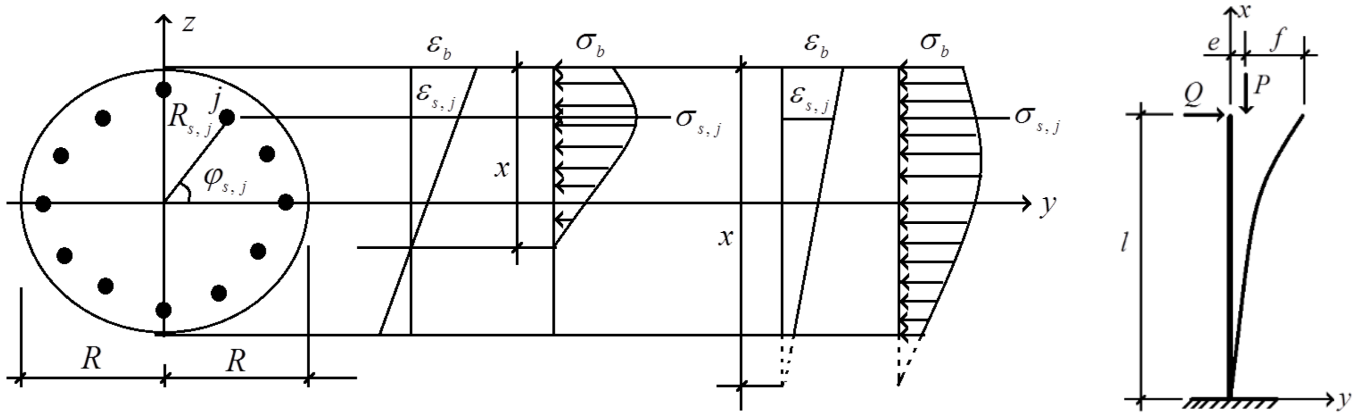

a) b)

Fig. 2. Computational scheme of cross-section (a) and cantilever support RC element (b)

Based on this relationship, the internal axial force and bending moment formed by the stresses in the reinforcement bars can be expressed as follows:

$$N_s\left(\varepsilon_b, x\right)=\sum_{j=1}^{K_s}\sigma_{s,j}\left(\varepsilon_b, x\right)\cdot A_{s,j}$$

$$M_s\left(\varepsilon_b, x\right)=\sum_{j=1}^{K_s}\sigma_{s,j}\left(\varepsilon_b, x\right)\cdot A_{s,j}\cdot R_{s,j}\cdot\sin\phi_{s,j} \tag{10}$$

Based on the obtained relationships, the equilibrium equations for the most stressed section can be written as follows:

$$N_b\left(\sigma_b, x\right)+N_s\left(\varepsilon_b, x\right)=P \tag{11}$$

$$M_b\left(\sigma_b, x\right)+M_s\left(\varepsilon_b, x\right)=P\left(e+f\right)+Q\cdot l \tag{12}$$

Thus, the main system of governing equations for solving the problem has been established. If we approximate the deflected axis of the compressed element within this system as $y(x)=f\cdot\tilde{y}(x)$ then, for the calculation of the separation in the section, the scheme can be written as $\chi=\varepsilon_b/x$ and $\chi=y''(x)=f\cdot\tilde{y}''(x_0)$. Here, x_0 is the abscissa of the most stressed section. From these two equations, the maximum deflection of the compressed element can be expressed in terms of the parameters ε_b and x as $f=\rho_0\cdot\dfrac{\varepsilon_b}{x}$. Here, $\rho_0=\dfrac{1}{\tilde{y}''(x_0)}$. For example, for a cantilever beam, if we take $\tilde{y}(x)=1-\cos\dfrac{\pi\cdot x}{2l}$ then $\rho_0=\dfrac{4l^2}{\pi^2}$. Therefore, the obtained nonlinear governing equation system (11) and (12) can be solved uniquely with respect to the parameters ε_b and x.

It should be noted that determining the stress–strain state and bearing capacity of circular cross-section compressed reinforced concrete elements under short-term static loading is also of significant practical interest. Therefore, this problem is addressed here as well. In this case, the governing nonlinear system of equations consists of equilibrium equations (11) and (12), together with the initial condition derived from equation (3), forming equation

$$\varepsilon_b=\frac{1}{E_b}\cdot U\left(\sigma_b\right) \tag{13}$$

A numerical solution algorithm for this system has been proposed [8,10]. Let us denote the horizontal force as H. By eliminating the force parameters from equations (11) and (12), the following relationship is obtained:

$$\begin{aligned}\Psi(x)&=M_b\left(\sigma_b, x\right)+M_s\left(\varepsilon_b, x\right)+\\&-\left(N_b\left(\sigma_b, x\right)+N_s\left(\varepsilon_b, x\right)\right)\cdot\left(e+\rho_0\cdot\frac{\varepsilon_b}{x}+\nu\cdot l\right)=0\end{aligned} \tag{14}$$

Since the variation interval of the σ_b stress parameter is known in advance, its value can be selected from this range. Consequently, the values of the associated parameters (ε_b and n_σ) become known, and equation (14) transforms into a single-variable nonlinear equation with respect to the x parameter that defines the position of the neutral axis. The root of this equation can be computed easily. Thus, for the accepted stress value (σ_b, ε_b, n_σ, x, f), the corresponding solutions are obtained. By varying the stress incrementally, all parameters characterising the stress–strain state can be determined without difficulty. Most importantly, this approach enables the construction of load–displacement diagrams, which are crucial for determining the bearing capacity of compressed elements.

5. Parametric study 2. Load–displacement behaviour of circular RC elements under short-term static loading

A computational module implementing the proposed solution algorithm has been developed, and parametric studies have been carried out to validate its effectiveness. As shown in Fig. 2, the RC element is made of B20-grade concrete, with a height of l = 9 m, a cross-sectional radius of R = 0.2 m, and reinforced uniformly with 12 bars distributed along the section. Under a condition of nominal central compression, i.e., with a random eccentricity of e = 1 sm, the stress–strain state and bearing capacity of the element were investigated for different reinforcement layouts. The results are presented in Fig. 3. According to Fig. 3, it is evident that under nominal central compression, the "load–displacement" curves exhibit descending branches, indicating that the bearing capacity of the element is governed by stability conditions rather than material strength alone. For the three reinforcement configurations considered, the ultimate load-bearing capacities were found to be $P_{ult(12\varnothing 28)}$ = 1124.2 kN, $P_{ult(12\varnothing 32)}$ = 1215.1 kN, and $P_{ult(12\varnothing 36)}$ = 1315.0 kN, respectively. Correspondingly, at the point of loss of bearing capacity, the maximum free-end displacement s of the element were $f_{ult(12\varnothing 28)}$ = 55.54 mm, $f_{ult(12\varnothing 32)}$ = 54.94 mm and $f_{ult(12\varnothing 36)}$ = 52.52 mm. Additionally, the compressive stresses in the most stressed section of the concrete face were recorded as $\sigma_{b,ult(12\varnothing 28)} = \sigma_{b,ult(12\varnothing 32)} = \sigma_{b,ult(12\varnothing 36)}$ = 11.9 MPa for the respective cases.

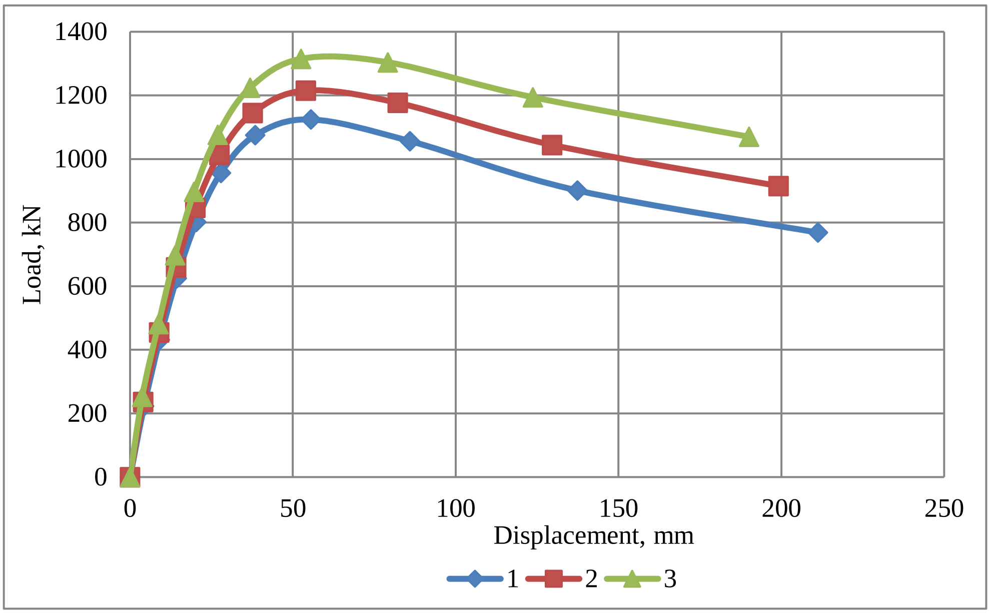

Fig. 3. Load–displacement curve of RC element under short-term static loading: 1 - 12∅28, 2 - 12∅32, 3 - 12∅36

6. Parametric study 3. time-dependent creep coefficient in RC elements

The developed computational module enables analysis of how various parameters affect the element's stress–strain state and bearing capacity. This capability is particularly important for determining initial conditions in the study of short-term critical loads and for evaluating the stress–strain behaviour under long-term loading when creep effects are considered. Under long-term loading, the governing system of equations for a selected time instant can be written as follows:

$$\begin{cases} \varepsilon_{bn} = \dfrac{1}{E_n} \cdot U(\sigma_{bn}) - \dfrac{\tau_n - \tau_{n-1}}{6} \cdot \left(K_{n,n} + 2 \cdot K^{*}_{n,n}\right) \cdot V(\sigma_{bn}) - W_n \\ N_b(\sigma_{bn}, x_n) + N_s(\varepsilon_{bn}, x_n) = P \\ M_b(\sigma_{bn}, x_n) + M_s(\varepsilon_{bn}, x_n) = P \cdot \left(e + \rho_{*} \cdot \dfrac{\varepsilon_{bn}}{x_n} + \nu \cdot l\right) \end{cases} \tag{15}$$

This nonlinear system of equations is solved using the previously described computational algorithm, allowing the determination of all parameters characterising the stress–strain state at any selected time instant. It becomes evident that, under long-term loading – where nonlinear hereditary creep of concrete is considered, the solution reduces to a sequence of short-term static problems evaluated at discrete time steps. This approach simplifies implementation and ensures accurate prediction of stress, strain, and evolution of displacement over time. A dedicated software module has been developed to implement this algorithm, and its application can form the basis of a separate research study.

In design codes, the effect of concrete creep is considered by reducing its elastic modulus using a creep coefficient. Thus, under long-term loading, instead of the elastic modulus, the calculation formulas include the modified modulus $\dfrac{E_{bt}}{1+\phi_{t,t_0}}$. Here, ϕ_{t,t_0} is the creep-adjusted modulus. This modulus is usually determined based on creep criteria under constant stress. It should be noted that in this case, the integral equation for nonlinear hereditary creep of concrete is replaced by a modified dependence similar to that used for short-term loading.

$$\varepsilon_{bt} = \left(1+\phi_{t,t_0}\right) \cdot \frac{\sigma_{bt}}{E_{bt}} \cdot \left[1 + \eta_1 \cdot \left(\frac{\sigma_{bt}}{R_b}\right)^{m_1}\right] \tag{16}$$

where ϕ_{t,t_0} is the creep coefficient, usually determined from creep curves under constant stress. In this simplified approach, the integral hereditary creep equation is replaced by a modified short-term relation. The value of ϕ_{t,t_0} can be obtained from relaxation analysis, and from equation (16), the following expression for the creep coefficient is proposed:

$$\phi_{t,t_0} = \frac{E_{bt}\cdot\varepsilon_{bt}}{\sigma_{bt}\cdot\left[1+\eta_1\cdot\left(\dfrac{\sigma_{bt}}{R_b}\right)^{m_1}\right]} - 1 \tag{17}$$

Consequently, for any selected t time instant, the governing system of equations can be written as:

$$\begin{cases} \varepsilon_{bt} = \left(1+\phi_{t,t_0}\right)\cdot\dfrac{\sigma_{bt}}{E_{bt}}\cdot\left[1+\eta_1\cdot\left(\dfrac{\sigma_{bt}}{R_b}\right)^{m_1}\right] \\ N_{bt}\left(\sigma_{bt}, x_t\right) + N_{st}\left(\varepsilon_{bt}, x_t\right) = P \\ M_{bt}\left(\sigma_{bt}, x_t\right) + M_{st}\left(\varepsilon_{bt}, x_t\right) = P\cdot\left(e+\rho_0\cdot\dfrac{\varepsilon_{bt}}{x_t}+\nu\cdot l\right) \end{cases} \tag{18}$$

This formulation enables the practical computation of the stress–strain state under long-term loading while incorporating creep effects in a simplified yet sufficiently accurate manner. Thus, by considering the nonlinear hereditary creep of concrete, the solution of the problem for different time instants is reduced to solving a series of short-term static-loading problems. This nonlinear system of equations was solved numerically using the algorithm described above, and the solution procedure can be easily implemented in software.

In this study, a dedicated computational module has been developed, and parametric studies have been conducted using it. Initially, the variation of the creep coefficient was determined. Figure 4 shows the relationship between the creep coefficient for B30-grade concrete and different loading times and initial stress conditions, with parameters E_{b0} = 32500 MPa, m_1 = 4.3, η_1 = 1.3, α_E = 0.573, β_E = 0.063 (day)$^{-1}$. From this figure, it is evident that one of the most influential factors affecting the maximum value of the creep coefficient is the age of the concrete. The influence of the initial stress level on the maximum value of the creep coefficient is very weak.

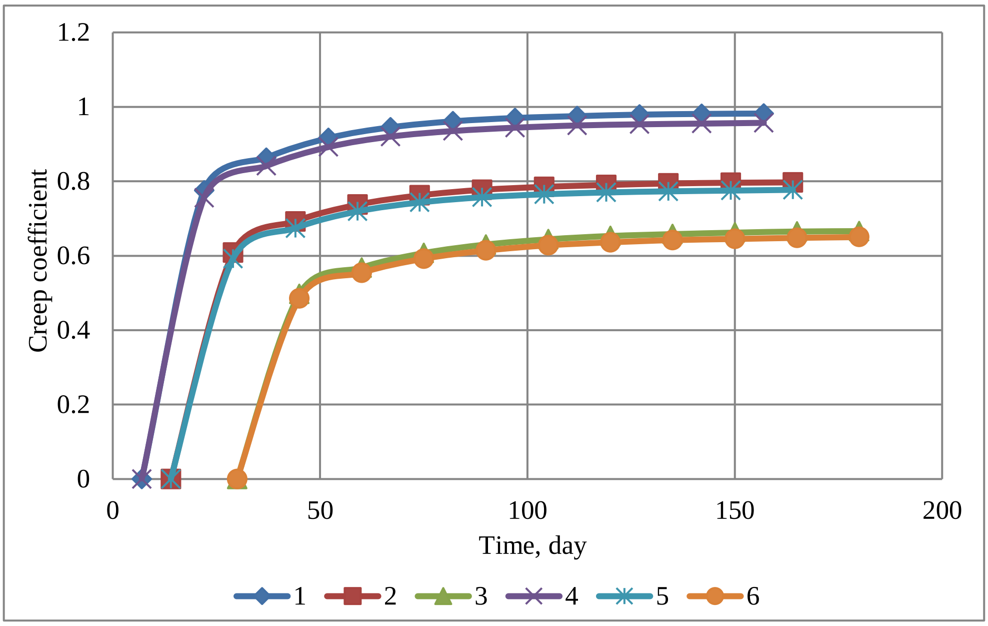

Fig. 4. Variation of the creep coefficient over time. 1 - t_0 = 7 day; $\sigma_{b0} = 0.5R_b$; 2 - t_0 = 14 day; $\sigma_{b0} = 0.5R_b$; 3 - t_0 = 30 day; $\sigma_{b0} = 0.5R_b$; 4 - t_0 = 7 day; $\sigma_{b0} = 0.85R_b$; 5 - t_0 = 14 day; $\sigma_{b0} = 0.85R_b$; 6 - t_0 = 30 day; $\sigma_{b0} = 0.85R_b$

7. Parametric study 4. Load-bearing capacity of compressed RC elements under short- and long-term hereditary creep

While examining the effect of concrete creep on the stress–strain state and bearing capacity of compressed elements, the analysis focuses on both short-term and long-term loading conditions. The element considered has a cross-sectional radius of R = 0.2 m, a height of l = 9 m, is made of B30-grade concrete, and reinforced with 12 bars of A400-grade steel. The stress–strain state under nominal central compression was investigated. Results of the parametric studies are presented in Fig. 5 as "load–displacement" curves. Curves 1, 3, 5 shows short-term static loading (without creep), while curves 2, 4, 6: Long-term static loading (with creep considered). All curves start at the origin and rise steeply, indicating the initial elastic response of the element. This phase is dominated by the stiffness of concrete and reinforcement, with minimal time-dependent effects. For short-term loading (curves 1, 3, 5), the maximum load-bearing capacity reaches $P_{ult(7)}$ = 1045.9 kN for the best reinforcement configuration. When creep is considered (curves 2, 4, 6), the peak load decreases significantly. For example, curve 6 shows a reduction from about $P_{ult(7)}$ = 1045.9 kN to $P_{ult(7,\infty)}$ = 824.6 kN, corresponding to a 21.2% decrease in bearing capacity due to creep. After reaching the peak, all curves exhibit a descending branch, which reflects loss of stability rather than material failure alone. This descending trend is more pronounced in long-term loading cases, indicating that creep accelerates instability and deformation growth. Short-term loading curves show ultimate displacement s around 150–180 mm while long-term loading curves extend further, up to 250 mm, demonstrating that creep significantly increases deformation before collapse.

These once again show that the load-bearing capacity of RC structural elements, especially compressed elements, should be calculated taking creep into account. According to load–displacement curve in shown Fig. 5, when t_0 = 14 day, $P_{ult(14)}$ = 1109.3 kN and $P_{ult(14,\infty)}$ = 907.1 kN, and when t_0 = 30 day, $P_{ult(30)}$ = 1189.5 kN and $P_{ult(30,\infty)}$ = 994.3 kN is obtained.

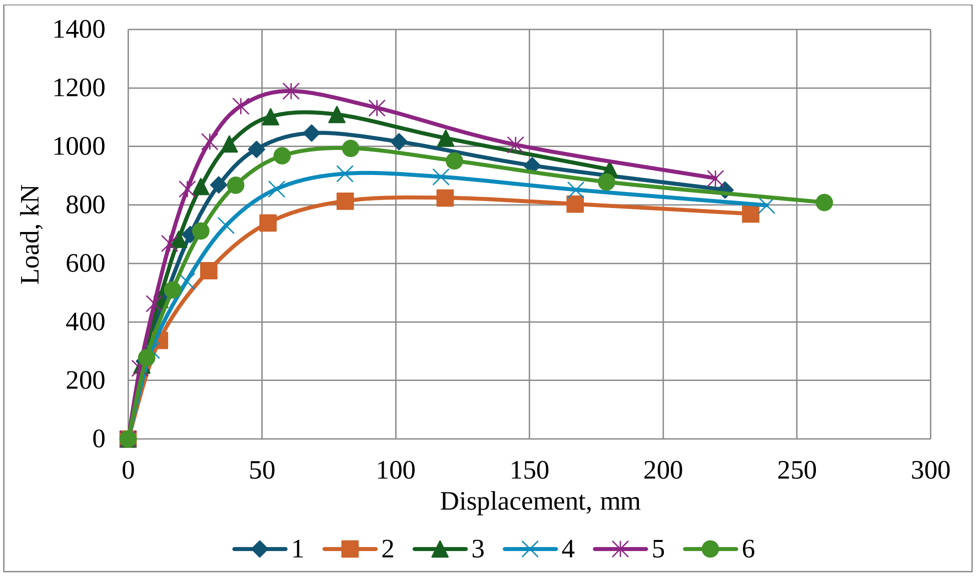

Fig. 5. Load–displacement curve of RC element considering concrete creep: 1 – t_0 = 7 day short-term loading; 2 – t_0 = 7 day long-term loading; 3 – t_0 = 14 day short-term loading; 4 – t_0 = 14 day long-term loading; 5 – t_0 = 30 day short-term loading; 6 – t_0 = 30 day long-term loading

8. Conclusions

- An efficient numerical methodology was developed to investigate the stress–strain state and bearing capacity of circular cross-section RC elements under short-term static loading, considering the nonlinear incomplete stress–strain diagram of concrete and the elastic–plastic behaviour of reinforcement. Unlike normative approaches, the proposed method does not require classifying elements as "short" or "long" or differentiating based on eccentricity magnitude, making it universally applicable.
- Parametric studies have confirmed that the bearing capacity of compressed elements is primarily governed by stability criteria rather than material strength alone.
- A discrete analogue of the nonlinear hereditary creep equation for concrete was formulated, enabling the incorporation of creep effects into the calculations. This approach reduces long-term analysis to a sequence of short-term static problems evaluated at different time intervals.
- A method for determining the creep coefficient from relaxation analysis was proposed and validated through parametric studies. It was established that the coefficient is weakly dependent on the stress level but strongly influenced by the loading age.
- Nonlinear creep of concrete significantly affects the performance of compressed reinforced concrete elements. The examined cases demonstrated that creep can reduce the bearing capacity by approximately 30%, underscoring the necessity of considering time-dependent effects in the design.
- The proposed computational methodology provides a unified framework for analysing the influence of various parameters on the stress–strain state and bearing capacity of RC elements under both short- and long-term loading conditions.

References

[1] Hajiyeva U.M., Study of the load-bearing capacity of compressed reinforced concrete elements based on tabular diagrams. *AzMIU Scientific Works* 2 (2021) 67-76 (in Azeri).

[2] Kolmogorov A.G., Plevkov V.S., *Calculation of reinforced concrete structures according to Russian and international standards*, Moscow, ASV, 2014 (in Russian).

[3] *SP 63.13330.2012. Code of Practice. Concrete and Reinforced Concrete Structures. Basic Provisions*. Updated Version of SNiP 52-01-2003. Moscow, Consultant Plus, 2013 (in Russian).

[4] Babich V.I., Kochkarov D.V., Calculation of reinforced concrete elements using the deformation method. *Concrete and Reinforced Concrete* 2 (2014) 12–16 (in Russian).

[5] Golyshev A.B., Kolchunov V.I., Yakovenko I.A., *Theory and calculation of reinforced concrete structures taking into account long-term processes*. Kiev, Talkom, 2015 (in Ukrainian).

[6] Kodysh E.M., Nikitin I.K., Trekin N.R., *Calculation of reinforced concrete structures made of heavy concrete for strength, crack resistance and deformations*. Moscow, ASV, 2010 (in Russian).

[7] Beglov A.D., Sanzharovsky R.S., *European standards and nonlinear theory of reinforced concrete*. Saint Petersburg, 2011 (in Russian).

[8] Hajiyev M., Damirov M., Stress-strain state and bearing capacity of compressed reinforced concrete elements of annular section. *Architectural Studies* 2(9) (2023) 35–46. https://doi.org/10.56318/as/2.2023.35

[9] Sanzharovsky R.S., Manchenko M.M., Nonlinear theory of concrete and reinforced concrete creep and modern standards, *Structural Mechanics of Engineering Structures and Buildings* 1 (2017) 23–35 (in Russian).

[10] Gadjiyev M.A., Guseynov I.G., Gadjiyeva U.M., Stress-strain state and load ability of compressed pipe-concrete elements, *SOCAR Proceedings* 1 (2023) 21–26. https://doi.org/10.5510/OGP2023SI100836

[11] Civier L., Chevillotte Y., Bles G., Montel F., Davies P., Marco Y., Short- and long-term creep behaviour of polyamide ropes for mooring applications, *Ocean Engineering* 259 (2022) 111800. https://doi.org/10.1016/j.oceaneng.2022.111800

[12] Le Roy R., Le Maou F., Torrenti J.M., Long term basic creep behavior of high-performance concrete: Data and modelling, *Materials and Structures* 50(1) (2017) 85. https://doi.org/10.1617/s11527-016-0948-8

[13] Reybrouck N., Van Mullem T., Taerwe L., Caspeele R., Influence of long-term creep on prestressed concrete beams in relation to deformations and structural resistance: Experiments and modelling, *Structural Concrete* 21(4) (2020) 1458–1474. https://doi.org/10.1002/suco.201900328

[14] Hajiyev M.A., Aeinehchi S., Bashirzade S.R., Asadov E.., Khalilov H.A., Study on the flexural performance of reinforced concrete structures strengthened with composites, *Engineering Mechanics* 8(16), (2024). 44-55. https://engineeringmechanics.az/uploads/2025/02/9-hajiyev-m-a-aeinehchi-s-bashirzade-s-r-asadov-e-z-khalilov-h-a.pdf

[15] Silva R.V., De Brito J., Dhir R.K., Comparative analysis of existing prediction models on the creep behaviour of recycled aggregate concrete, *Engineering Structures* 100 (2015) 31–42. https://doi.org/10.1016/j.engstruct.2015.06.004

[16] Kammouna Z., Briffaut M., Malecot Y., Experimental study of the creep effect on the mechanical properties of concrete, *Advances in Civil Engineering* 2019(1) (2019) 5907923. https://doi.org/10.1155/2019/5907923

[17] Daou H., Raphael W., Geara F., Evaluation of factors affecting long-term creep of concrete using machine learning regression models. In *Bridge Safety, Maintenance, Management, Lifecycle, Resilience and Sustainability*, CRC Press, 2022, 1197–1204.

[18] Bondarenko V.M., Bondarenko S.V., *Engineering methods of nonlinear theory of reinforced concrete*, Stroyizdat, Moscow, 1982 (in Russian).

[19] Livshits Y.D., *Calculation of reinforced concrete structures taking into account the effects of shrinkage and creep*, Vishcha School, Kyiv, 1976 (in Russian).